

CONCOMITANT ACTIVATION OF TWO TYPES OF GLUTAMATE RECEPTOR MEDIATES EXCITATION OF SALAMANDER RETINAL GANGLION CELLS

BY SCOTT MITTMAN, W. ROWLAND TAYLOR*
AND DAVID R. COPENHAGEN

*From the Department of Ophthalmology, Box 0730, University of California,
San Francisco, CA 94143, USA*

(Received 1 December 1989)

SUMMARY

1. Cells in the ganglion cell layer of salamander retinal slices were voltage clamped using patch pipettes. Light elicited transient excitatory postsynaptic currents (EPSCs) in on-off ganglion cells and sustained EPSCs in on ganglion cells. Light-evoked inhibitory postsynaptic currents in these cells could be blocked by 100 μ M-bicuculline methobromide and 500 nM-strychnine.

2. In the presence of external Cd^{2+} , at a concentration that blocked light-evoked synaptic inputs, *N*-methyl-D-aspartate (NMDA) and the non-NMDA-receptor agonists, quisqualate and kainate, gated conductances in both on-off and on ganglion cells. The current-voltage (*I*-*V*) curve for the conductance elicited by NMDA had a negative slope between -40 and -70 mV and a reversal potential near 0 mV. The *I*-*V* curves for the non-NMDA-receptor-mediated conductances were nearly linear and also had reversal potentials near 0 mV.

3. *I*-*V* curves were measured at an early time point near the peak of transient EPSCs and at a later time point during the decay phase of the responses. The late *I*-*V* curve had a negative slope below -40 mV. The early *I*-*V* curve had a positive slope over the entire voltage range but the slope was greater at positive than at negative potentials. The evoked current reversed near 0 mV at both time points.

4. The region of negative slope of the late *I*-*V* curve was eliminated when Mg^{2+} was removed from the external saline. A slowly decaying component of transient EPSCs was eliminated in 20 μ M-DL-2-amino-7-phosphonoheptanoate (AP7), an NMDA-receptor antagonist.

5. Application of 1 μ M-6-cyano-7-nitroquinoxaline-2,3-dione (CNQX), a non-NMDA-receptor antagonist at this concentration, blocked a fast component of transient EPSCs.

6. Our results demonstrate that the synaptic inputs to on-off ganglion cells have two components: a slower NMDA-receptor-mediated component having a time-to-peak of 110 ± 45 ms and an e-fold decay time of 209 ± 35 ms at -31 mV (mean \pm s.d.,

* Present address: Department of Neurobiology D-238, Stanford University School of Medicine, Stanford, CA 94305, USA.

$n = 5$), and a faster non-NMDA-receptor-mediated component having a time-to-peak of 28 ± 10 ms and an e-fold decay time of 43 ± 20 ms at -31 mV ($n = 8$).

7. A similar analysis of sustained EPSCs of on ganglion cells showed that these currents resulted from sustained activation of both NMDA and non-NMDA receptors.

INTRODUCTION

Glutamate is the leading candidate for the transmitter mediating excitation of vertebrate retinal ganglion cells (Slaughter & Miller, 1983*a*; Coleman, Massey & Miller, 1986). Glutamate and other acidic amino acid-receptor agonists excite retinal ganglion cells of rabbit, rat and mudpuppy by activating both *N*-methyl-D-aspartate (NMDA) and non-NMDA receptors in the membranes of these cells (Slaughter & Miller, 1983*b*; Lukasiewicz & McReynolds, 1985; Coleman *et al.* 1986; Aizenman, Frosch & Lipton, 1988; Massey & Miller, 1988). Furthermore, a number of non-specific acidic amino acid-receptor antagonists, such as (\pm)*cis*-2,3-piperidine dicarboxylate, kynurenate and *D*-*O*-phosphoserine, block light-evoked responses of ganglion cells (Slaughter & Miller, 1983*a*; Coleman *et al.* 1986; Massey & Miller, 1988; Coleman & Miller, 1989) suggesting that these receptors mediate light responses.

In spite of clear evidence that NMDA receptors are found in ganglion cell membranes, the role of these receptors is uncertain. Some studies have suggested that NMDA receptors are non-synaptic and play little or no role in light-evoked responses (Slaughter & Miller, 1983*b*; Coleman *et al.* 1986; Massey & Miller, 1988; Coleman & Miller, 1988; Coleman & Miller, 1989). Other studies have concluded that NMDA receptors mediate part of the response of on, but not on-off, ganglion cells in mudpuppy retina (Lukasiewicz & McReynolds, 1985).

At other synapses in the nervous system, voltage-clamp methods have proved useful in identifying NMDA- and non-NMDA-receptor-mediated synaptic inputs to postsynaptic neurones. It has been shown that excitatory postsynaptic potentials and currents (EPSPs and EPSCs) consist of a fast, non-NMDA-receptor-mediated component and a slower, NMDA-receptor-mediated component (Dale & Roberts, 1985; Wigström, Gustafsson & Huang, 1985; Forsythe & Westbrook, 1988; Bekkers & Stevens, 1989).

We have voltage clamped cells in the ganglion cell layer of the tiger salamander retina and have investigated the kinetics and pharmacology of light-evoked EPSCs in on-off and on cells. Light-evoked EPSCs consist of fast and slow components mediated by non-NMDA and NMDA receptors, respectively.

METHODS

Retinal slices

Neotenus tiger salamanders (*Ambystoma tigrinum*), 20–30 cm in length, were maintained in tap water at 2 °C. Light from a 100 W incandescent bulb, 1–2 m distant from the animals, was present for 12 of every 24 h. Animals were transferred to darkness at least 1 h prior to decapitation and double-pithing. Retinal slices, 150 μ m thick, were prepared as described by Werblin (1978) and Wu (1987), except that all procedures were done under dim 700 nm illumination.

Superfusion

The experimental chamber was functionally similar to that described by Wu (1987). Saline, at room temperature (20–22 °C), flowed through the 600 μl chamber at a rate of 700 $\mu\text{l min}^{-1}$. Salamander saline consisted of 104 mM-NaCl, 2 mM-KCl, 2 mM-CaCl₂, 1 mM-MgCl₂, 5 mM-glucose and 5 mM-HEPES, adjusted to pH 7.6 with NaOH. Saline components were of reagent grade.

Light evoked both EPSCs and inhibitory postsynaptic currents (IPSCs) in ganglion cells. The excitatory and inhibitory components of light responses overlapped considerably (Fig. 4). Thus, the control saline in the majority of experiments (all figures, except Figs 1, 4A and B), also contained 500 nM-strychnine hydrochloride and 100 μM -bicuculline methobromide (both from Sigma) to block IPSCs.

In experiments examining the actions of acidic amino acid-receptor agonists (Figs 2 and 3), 20 μM -CdCl₂ was added to the control saline to eliminate indirect agonist effects by blocking synaptic transmission. Light-evoked activity in these experiments was recorded prior to addition of Cd²⁺ and agonist-evoked responses were recorded after at least 5 min of Cd²⁺ superfusion.

Mg²⁺-free saline (Fig. 6) was prepared by omitting MgCl₂.

Acidic amino acid-receptor antagonists were applied by addition to the control saline. Their effects were determined after at least 4 min of superfusion and they were allowed to wash out for at least 10 min prior to recovery runs. DL-2-Amino-7-phosphonoheptanoic acid (AP7) was purchased from Cambridge Research Biochemicals; 6-cyano-7-nitroquinoxaline-2,3-dione (CNQX), from Tocris Neuramin.

Patch pipettes and recordings

Patch pipettes for tight-seal, whole-cell recording (Marty & Neher, 1983) were pulled from capillary tubing made of Corning 8161 glass (Garner Glass). Pipette tapers were coated with Sylgard 184 silicone elastomer (Dow Corning); pipettes were not fire-polished. The bubble pressure of the pipettes (Mittman, Flaming, Copenhagen & Belgum, 1987) was between 90 and 110 kPa, measured in acetone.

The pipette solution in the majority of experiments consisted of 84 mM-CsF, 3.4 mM-NaCl, 400 μM -MgCl₂, 400 μM -CaCl₂, 11 mM-EGTA, 10 mM-NaHEPES, adjusted to pH 7.6 with CsOH. For cells in which both voltage- and current-clamp recordings were performed (Fig. 1), K⁺ replaced Cs⁺ as the predominant cation of the pipette solution. Fluoride was chosen as the predominant anion of the pipette solution because it greatly increased the yield of high-quality recordings. Because of the low solubility of MgF₂ (solubility product = 7.1×10^{-9}), the free Mg²⁺ concentration of the pipette solution was calculated to be about 1 μM .

An Axopatch 1A amplifier (Axon Instruments) was used for recordings. The ground terminal of the amplifier contacted the superfusing saline via a Ag–AgCl pellet and a 3 M-KCl–agarose bridge; the connection between pipette solution and amplifier was via a second Ag–AgCl pellet.

The cells selected for recording were large cells in the ganglion cell layer whose cell bodies were exposed to the surface of the slice and whose nuclei were not granular in appearance. Up to 50% of cells in the ganglion cell layer may be displaced amacrine cells (Turner, Delaney & Powell, 1978; Ball & Dickson, 1983). We have not developed criteria for discriminating between ganglion cells and displaced amacrine cells. However, in retinas of other species, the ganglion cells have been found to be the larger of the two cell types (Perry, 1979). If this dichotomy holds for tiger salamander, our sample would be biased in favour of ganglion cells.

The seal conductance between pipette and cell membrane prior to the rupture of the patch was usually less than 300 pS. No enzymatic treatment of the slices was necessary. Seals formed quickly after application of a transmural pressure of –4.5 to –12 kPa. The fast capacitance compensation was adjusted to cancel the transient caused by the capacitance of the pipette. We could not electronically compensate for the series conductance of the pipette or the cell membrane capacitance because of the anisopotentiality of retinal ganglion cells. In seventeen recordings in which the electrical behaviour of the cells was analysed in detail, the series conductance was found to be 42 ± 32 nS (mean \pm s.d.). A detailed consideration of voltage-clamp errors arising from pipette series conductance and ganglion cell anisopotentiality will be published elsewhere (W. R. Taylor, S. Mittman & D. R. Copenhagen, in preparation). Signals passed through a 4-pole low-pass Bessel filter with a cut-off (–3 dB) frequency of 500 Hz for current recordings and 1 kHz for voltage recordings. Signals were usually sampled at 1 kHz. Voltages have been corrected by –6 mV for the

change in liquid junction potential at the pipette tip resulting from establishment of a whole-cell recording.

Light stimulation

Light stimuli were delivered at a right angle to the long axis of the photoreceptors via the microscope condenser, a Fluor 20× lens (Nikon). The light source was a 100 W tungsten quartz iodine lamp, filtered by a 520 nm interference filter and a variable number of neutral density filters. The photon density of the stimulus, unattenuated by neutral density filters, was 2×10^{20} photons $\text{m}^{-2} \text{s}^{-1}$. The stimulus illuminated a 690 μm stretch of the slice centred on the selected ganglion cell. As the diameter of the receptive field centre of retinal ganglion cells in eye-cup preparations of tiger salamander is between 400 and 1000 μm (Wunk & Werblin, 1979), it is presumed that the stimulus used here excited primarily the receptive field centres. The same light source and 520 nm interference filter were used for illumination during cell selection and pipette placement, but a slit was inserted into the optics at a plane conjugate to the Hoffman modulator in the 40× water-immersion objective, as described by Hoffman & Gross (1975).

Agonist application

Acidic amino acid-receptor agonists (from Sigma) were applied by ionophoresis, by pressure ejection or by addition to the superfusing saline. Ionophoretic pipettes (20–30 M Ω , if filled with 3 M-KCl) contained 500 mM, pH 8 solutions of agonists and were positioned a few micrometres above the inner plexiform layer within 40 μm of the recorded ganglion cell soma. Pressure ejection pipettes (acetone bubble pressure of 70–100 kPa) contained solutions of agonists dissolved in the superfusing saline (which always included 20 μM -CdCl₂ during agonist application) and were positioned 25 μm above the distal edge of the ganglion cell soma.

Non-synaptic currents of ganglion cells

Changes in potential from a holding potential of -60 mV evoked transient currents which had largely subsided after 500 ms (Lukasiewicz & Werblin, 1988); these will be termed non-synaptic currents. Light and agonist stimuli were thus applied at least 500 ms after clamp potential changes. Under our recording conditions the amplitude of the steady-state non-synaptic conductances was smaller than or comparable to the light-activated conductances (data not shown).

Normalization of currents

Approximately equal numbers of experiments were performed with a series of ten clamp potentials starting at -111 mV and separated by 15 mV and with a series of ten clamp potentials starting at -106 mV and separated by 15 mV. The use of different clamp potentials and the natural variation in the amplitude of currents necessitated normalization of currents for the construction of current-voltage (I - V) curves in Figs 2, 3 and 5–7.

A normalized I - V curve is defined as

$$\frac{G^*}{G_i} I_i(V),$$

where $I_i(V)$ is the i^{th} raw I - V curve, G_i is the slope of the line which best fits $I_i(V)$ over some range of V and G^* is a scale factor.

G_i values were calculated for $V \geq -6$ mV in Fig. 2 and for all values of V in Fig. 3. G^* was 1 ns. The conductance means and standard deviations cited in the legends of Figs 2 and 3 were calculated from the appropriate G_i .

For the experiments of Figs 5–7, mean, normalized I - V curves were calculated. In these experiments, responses from numerous cells were examined in three different conditions: pre-treatment, treatment and recovery. $I_{p,i}(V)$, $i = 1 \dots m$, denote the m raw I - V curves obtained in the pre-treatment condition with one set of potentials. Likewise, $I_{p',i}(V)$, $i = 1 \dots n$, denote the n raw I - V curves obtained in the pre-treatment condition with the second set of potentials. The raw I - V curves obtained in treatment and recovery conditions are denoted by $I_{t,i}(V)$, $I_{t',i}(V)$, $I_{r,i}(V)$ and $I_{r',i}(V)$.

Mean, normalized I - V curves were calculated as follows:

$$\bar{I}_x(V) = \frac{G^*}{m} \sum_{i=1}^m \frac{I_{x,i}(V)}{G_i},$$

$$\bar{I}_{x'}(V') = \frac{G^*}{n} \sum_{i=1}^n \frac{I_{x',i}(V')}{G'_i},$$

where x represents p , t or r . Slopes G_i and G'_i were calculated from I - V curves obtained in one condition and were used in the calculation of the mean, normalized I - V curves for all conditions. Thus, the I - V curves of Figs 5*B*, 6*B*, 7*B* and *C* were normalized using the slopes of the lines which best fitted $I_{p,i}(V)$ and $I_{p',i}(V')$ for $V, V' \geq -6$ mV. The I - V curves of Fig. 5*C* were normalized using the slopes of the lines which best fitted $I_{t,i}(V)$ and $I_{t',i}(V')$ for all values of V, V' . G^* was calculated as follows:

$$G^* = \frac{\sum_{i=1}^m G_i + \sum_{i=1}^n G'_i}{m+n}.$$

Standard deviations (σ) were calculated as follows:

$$\sigma_x(V) = \left\{ \frac{\sum_{i=1}^m \left[\frac{I_{x,i}(V)G^*}{G_i} - \bar{I}_x(V) \right]^2}{m} \right\}^{\frac{1}{2}},$$

$$\sigma_{x'}(V') = \left\{ \frac{\sum_{i=1}^n \left[\frac{I_{x',i}(V')G^*}{G'_i} - \bar{I}_{x'}(V') \right]^2}{n} \right\}^{\frac{1}{2}}.$$

This procedure allowed us to pool data obtained using different series of clamp potentials. This procedure also ensured that the slope conductance of the resulting plots represented the mean behaviour of the population of ganglion cells studied.

RESULTS

The light responses of on and on-off ganglion cells are distinct in both current- and voltage-clamp recordings

Recordings in eye-cup preparations have demonstrated three types of ganglion cell: on, on-off and off. These three classes remain obvious in slice preparations when recording either voltage or current responses. The top traces in Fig. 1 show examples of on-off (*A*) and on (*B*) ganglion cell voltage responses to a 2.5 s step increase in illumination. The on-off cell responded with a transient depolarization accompanied by a volley of action potentials at both the onset and cessation of the stimulus. The relative amplitudes of the on and off responses varied among cells. The on cell responded with a sustained depolarization accompanied by action potentials, which often showed accommodation of the spike rate. After periods in darkness, the first light response was often much larger than subsequent responses. Such adaptation effects were allowed for by ignoring the first several light responses after periods in darkness.

Voltage clamped near the resting potential, these same cells responded to the same stimulus with inward currents similar in time course to the voltage responses (Fig. 1*A* and *B*, bottom), indicating that the voltage responses were shaped primarily by synaptically activated conductances. Following Wunk & Werblin (1979), we term the responses of the on-off cell transient EPSCs and the response of the on cell a sustained EPSC.

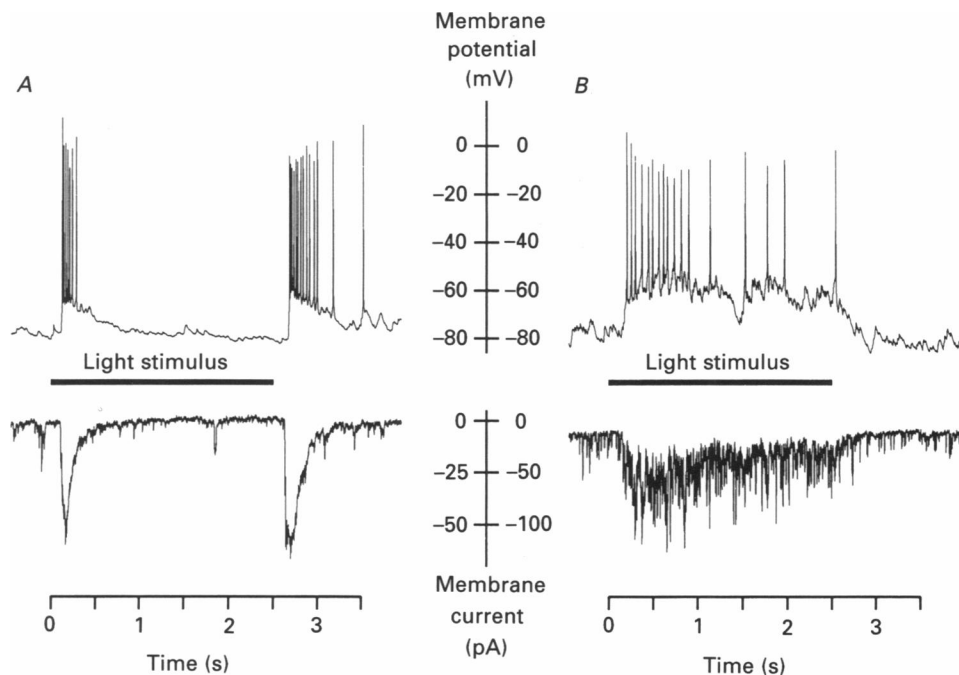


Fig. 1. Voltage (top traces) and current (bottom traces) responses to illumination of the receptive field centres of an on-off ganglion cell (*A*) and an on ganglion cell (*B*). Clamp potential for the bottom traces was -76 mV. The timing of the light stimuli is indicated by the bar. Photon densities were 6×10^{17} (*A*) and 6×10^{16} photons $\text{m}^{-2} \text{s}^{-1}$ (*B*). Slope conductances of the cells in darkness, at -76 mV: *A*, 770 pS; *B*, 590 pS.

On-off cells were the most frequently encountered ganglion cells. In a sample of ninety-four cells, eighty-one (86%) responded to illumination with transient EPSCs at onset and termination and the remaining thirteen (14%) cells responded with sustained EPSCs. Only a small number of off cells were encountered and no data on this class of cell are included.

NMDA- and non-NMDA-receptor-gated conductances are present on salamander retinal ganglion cells

Previous studies have shown that NMDA- and non-NMDA-receptor agonists excite ganglion cells in intact retinas of mudpuppy and rabbit and isolated ganglion cells of rat. We sought to extend these findings to ganglion cells of tiger salamander retina.

To ensure that the agonists were acting directly on the ganglion cells, and not through an intermediate neurone, synaptic transmission was blocked using $20 \mu\text{M}$ - Cd^{2+} , a concentration insufficient to block NMDA-receptor-mediated responses significantly (Mayer, Vyklicky & Westbrook, 1989). Figure 2*A* shows light-evoked EPSCs recorded at 19 s intervals after application of $20 \mu\text{M}$ - Cd^{2+} . After 5 min, synaptic transmission was completely suppressed. Figure 2*B* shows responses to subsequent ionophoretic applications of NMDA at a site in the inner plexiform layer, adjacent to the ganglion cell. Little inward current was elicited at the most negative potentials, but a large inward current was evident at -36 mV and this current

reversed close to 0 mV. Figure 2C shows that the *I-V* curves of NMDA-evoked responses had the region of negative slope conductance characteristic of such responses in other preparations (Mayer, Westbrook & Guthrie, 1984; Nowak, Bregestovski, Ascher, Herbet & Prochiantz, 1984; Mayer & Westbrook, 1985).

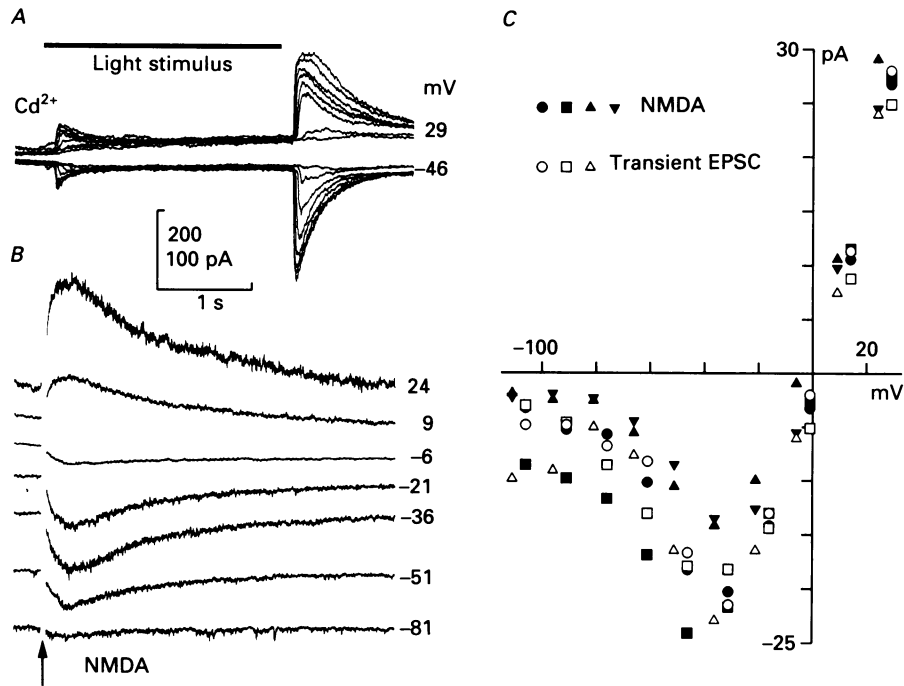


Fig. 2. *A*, responses during the first 5 min of superfusion with saline containing $20 \mu\text{M}$ - Cd^{2+} . Responses were recorded in alternation at the two potentials listed to the right of the traces. Cd^{2+} caused a progressive decline in amplitude. Light intensity was 6×10^{17} photons $\text{m}^{-2} \text{s}^{-1}$. *B*, currents evoked by ionophoresis ($\approx 5.6 \text{ nC}$) of NMDA. The arrow indicates the timing of the ionophoresis; the stimulus artifacts have been removed for clarity. *C*, normalized *I-V* curves of peak NMDA responses from four cells (\blacksquare and \bullet indicate addition to the superfusing saline and \blacktriangle indicate ionophoretic application). The matched open symbols show *I-V* curves of the slow component of transient EPSCs (measured 300–432 ms after cessation of light responses) in the same cells. The cell represented by \blacktriangledown had no light response. The raw *I-V* curves had mean slopes over this voltage range of $5.0 \pm 1.5 \text{ nS}$ ($n = 4$) for NMDA responses and $3.8 \pm 0.9 \text{ nS}$ ($n = 3$) for light responses. Current calibration: *A*, 200 pA; *B*, 100 pA.

Similar experiments using quisqualate (Fig. 3A) and kainate (Fig. 3B) indicated that these two agonists evoked currents with nearly linear *I-V* curves, typical of non-NMDA-receptor-gated conductances (Mayer & Westbrook, 1984).

I-V curves suggest that transient EPSCs consist of at least two components

Having demonstrated that NMDA and non-NMDA receptors, mediating conductances with distinct *I-V* curves, were present on ganglion cells, we sought to determine whether one or both of these receptors mediated the light-evoked excitatory synaptic inputs to these cells. Inspection of light-evoked currents at

different potentials revealed, however, that IPSCs with a reversal potential of about -55 mV (data not shown) largely obscured the EPSCs of many ganglion cells (Fig. 4A). The only evidence of excitatory input in these records was the biphasic off response at -31 mV.

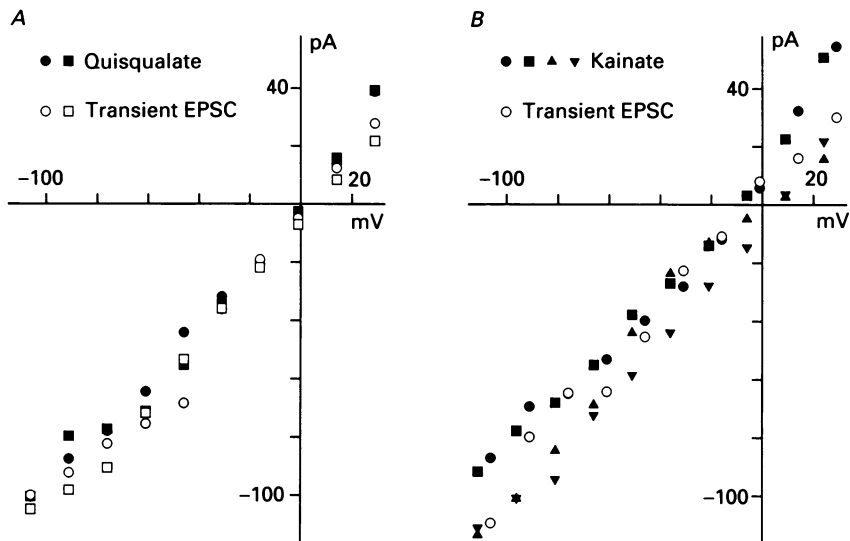


Fig. 3. *A*, normalized I - V curves of peak responses to quisqualate applied by pressure ejection (filled symbols) and of the fast component of transient EPSCs in these same cells (matched open symbols). *B*, normalized I - V curves of peak responses to kainate applied by pressure ejection (\bullet) or ionophoresis (\blacksquare , \blacktriangle and \blacktriangledown). One of these cells had a light response and the normalized I - V curve of the fast component of its off transient EPSC is plotted with open circles. The raw I - V curves had mean slopes of 880 ± 60 pS ($n = 2$) for quisqualate responses, 1.7 ± 0.6 nS ($n = 4$) for kainate responses and 2.7 ± 1.3 nS ($n = 3$) for light responses. The fast component of transient EPSCs was isolated by addition of $20 \mu\text{M}$ -AP7 to the saline. I - V curves of the fast component were measured 138–144 ms after cessation of light.

The inhibitory responses of ganglion cells have been shown to be mediated by GABA_A and glycine receptors (Miller, Dacheux & Frumkes, 1977; Frumkes, Miller, Slaughter & Dacheux, 1981; Miller, Frumkes, Slaughter & Dacheux, 1981; Belgum, Dvorak & McReynolds, 1984). Thus, we attempted to isolate EPSCs through the use of the antagonists bicuculline methobromide and strychnine. Addition of $100 \mu\text{M}$ -bicuculline methobromide to the salamander saline (Fig. 4B) abolished a portion of the inhibitory activity. The apparent reversal potentials of both the on and off responses shifted to more positive potentials. Further addition to the saline of 500 nM -strychnine (Fig. 4C) blocked the remainder of the inhibitory input; both on and off responses clearly reversed near 0 mV.

Both the time-to-peak and duration of transient EPSCs increased at more positive potentials (Fig. 4C). This behaviour was analysed by means of I - V curves, measured at two times during on or off transient EPSCs. An early I - V curve was measured near the time of the current peak at the most hyperpolarized potential, and is indicated in Fig. 4C by the open square. A late I - V curve was measured at a time when most

of the current had decayed at hyperpolarized potentials, but not at depolarized potentials (○). In Fig. 4D, the two *I-V* curves are plotted with symbols

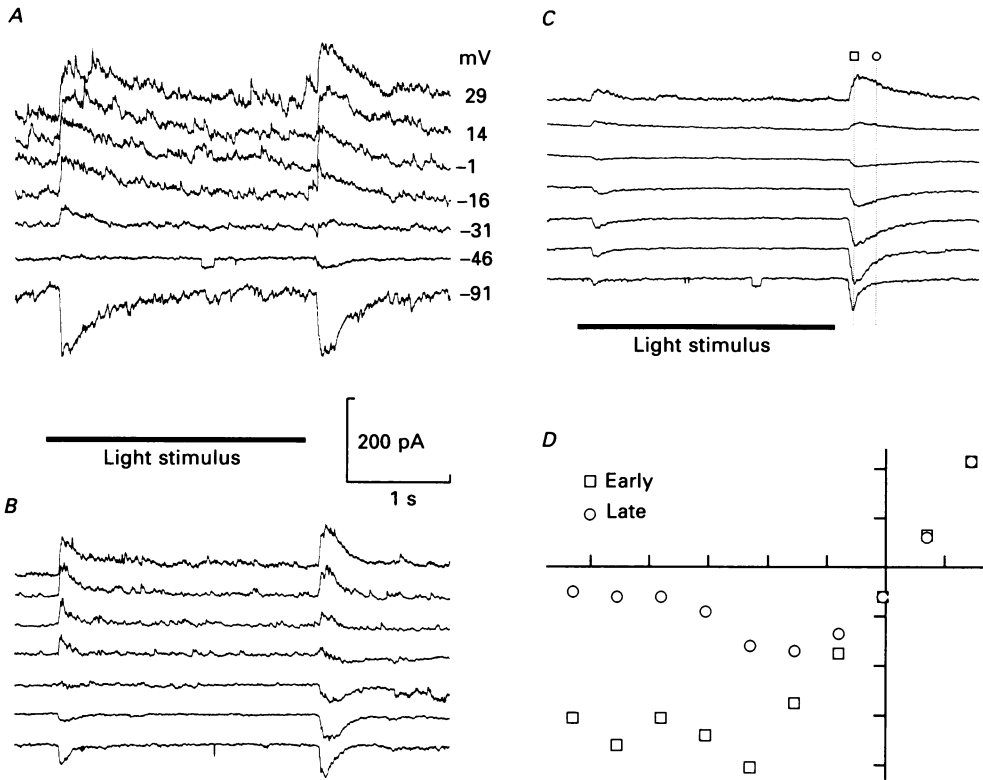


Fig. 4. Light-evoked postsynaptic currents of an on-off ganglion cell were recorded at the potentials listed to the right of each trace in three superfusion solutions: *A*, salamander saline; *B*, salamander saline + 100 μM-bicuculline methobromide; *C*, salamander saline + 100 μM-bicuculline methobromide + 500 nM-strychnine hydrochloride. The light stimulus (6×10^{17} photons $m^{-2} s^{-1}$) is indicated by the bar. *D*, the current evoked 184 ms (□) or 400 ms (○) after cessation of the light stimulus is plotted as a function of potential. Evoked current was calculated as the difference between current at the indicated time and current just prior to cessation of the light stimulus.

corresponding to those of Fig. 4C. Neither *I-V* curve was linear over the full range of potentials. The early *I-V* curve was fairly linear between 30 and -30 mV, but at more negative voltages the current remained nearly constant despite changes in voltage. The late *I-V* curve was relatively linear only between 30 and 0 mV. Between -30 and -75 mV, the *I-V* curve had a negative slope, characteristic of responses mediated by NMDA receptors.

The similarity of the *I-V* curve measured late in the light response to those of NMDA-evoked responses raised the possibility that a component of the light response was mediated by NMDA receptors. Furthermore, the differences between the early and late *I-V* curves suggested that NMDA-receptor activation predominated relatively late in the light response.

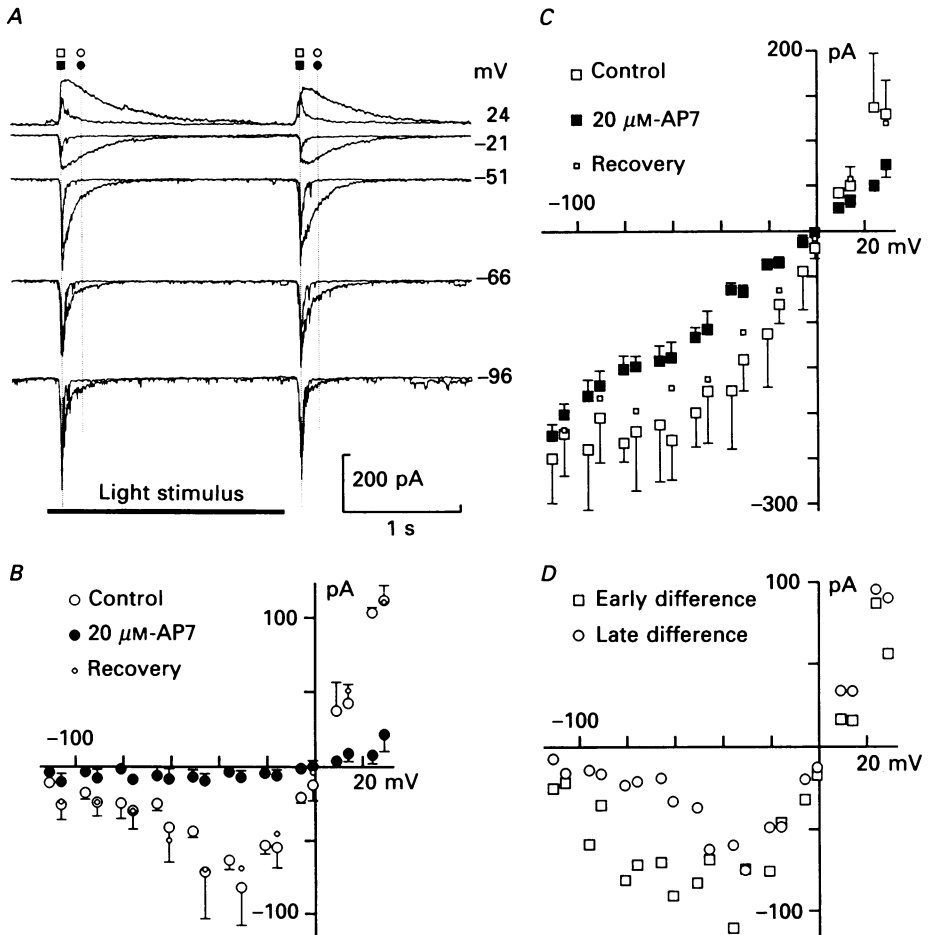


Fig. 5. *A*, transient EPSCs evoked by light (6×10^{17} photons $\text{m}^{-2} \text{s}^{-1}$) both before and during application of $20 \mu\text{M}$ -AP7. The control record is the more slowly decaying of each pair. *B*, mean, normalized late I - V curves from two on and ten off transient EPSCs. These I - V curves were measured at latencies of 250–450 ms from the onset or cessation of a light step. The actions of AP7 on on transient EPSCs were not obviously different from the actions on off transient EPSCs. *C*, mean, normalized, early I - V curves from the same transient EPSCs as in *B*. The I - V curves were measured at latencies of 103–168 ms from the onset or cessation of a light step. *D*, early (\square) and late (\circ) I - V curves of the AP7-resistant current, obtained by subtracting the AP7 I - V curves from the control I - V curves of *C* and *B*, respectively.

AP7 blocks a slowly decaying component of transient EPSCs

To test further the idea that a component of transient EPSCs was mediated by NMDA receptors, the NMDA-receptor antagonist AP7 (Olverman, Jones & Watkins, 1984) was applied at a concentration of $20 \mu\text{M}$. Figure 5*A* shows control transient EPSCs superimposed on those recorded in AP7. AP7 did not change the latency or rate of rise of EPSCs, but strongly suppressed a slowly decaying component which was more prominent at potentials above -60 mV. The AP7-resistant current had a

rapid time course at all potentials. There were no obvious differences in the effect of AP7 on on or off EPSCs.

The mean, normalized early and late I - V curves of twelve transient EPSCs (two on EPSCs, ten off EPSCs, in ten cells), measured in control solution and AP7 are shown in Fig. 5*B* and *C*. AP7 almost abolished the late current (Fig. 5*B*, ●). AP7 also blocked a portion of the early current (Fig. 5*C*), leaving a current with an essentially constant slope conductance (■). Figure 5*D* shows that the AP7-sensitive components measured early (□) and late (○) during transient EPSCs displayed the characteristic negative slope conductance of NMDA-receptor channels.

The effects of AP7 were fully reversible, as illustrated by the recovery I - V curves (small symbols) of Fig. 5*B* and *C*.

The negative slope conductance of the slow component of transient EPSCs is eliminated in Mg²⁺-free saline

The negative slope conductance of NMDA-receptor-gated currents is due to voltage-dependent block of the channels by external Mg²⁺ (Mayer *et al.* 1984; Nowak *et al.* 1984; Mayer & Westbrook, 1985). If the slow component of transient EPSCs was due to NMDA-receptor activation then the I - V curve of this component would become more nearly linear in Mg²⁺-free solutions. Figure 6*A* shows that, for both on and off responses, the slow component of transient EPSCs at hyperpolarized potentials was larger in Mg²⁺-free saline. Mean, normalized late I - V curves from fifteen cells are shown in Fig. 6*B*. The open circles show that the late I - V was more nearly linear and lacked a negatively sloped region in Mg²⁺-free saline. The residual non-linearity of the I - V curve was presumably due to trace Mg²⁺ in the solutions used (Mayer & Westbrook, 1987). Addition of 1 mM-Mg²⁺ to the saline restored the region of negative slope conductance (●). Upon removal of external Mg²⁺, this effect was reversed (small circles).

The voltage dependence of the Mg²⁺ block of the slow component was compared with previous results for an NMDA-gated conductance (Ascher & Nowak, 1988) by fitting a simple two-barrier, one-site model (Hille, 1984) to the data. These calculations are best done after blocking components of the light responses other than the slow component (see the results of the next section). The continuous line in Fig. 7*C* was calculated from a model (described in the figure legend) in which Mg²⁺ competes with monovalent ions for a single binding site within the membrane electrical field. The data are consistent with the Mg²⁺ binding site being near the inner surface of the membrane at a point 99% through the membrane electrical field. The K_d was 56 mM at 0 mV.

CNQX blocks the fast component of transient EPSCs

Experiments in which the slow component of transient EPSCs was blocked with AP7 revealed a fast component with a nearly linear I - V curve (Fig. 5*C*). Since quisqualate and kainate also elicit responses with linear I - V curves in these cells (Fig. 3*A* and *B*), we tested the hypothesis that the fast component of transient EPSCs may be mediated by non-NMDA receptors.

Application of 1 μM-CNQX, a specific antagonist of non-NMDA receptors (Honoré, Davies, Drejer, Fletcher, Jacobsen, Lodge & Nielsen, 1988; Yamada, Dubinsky &

Rothman, 1989), selectively suppressed the fast component of transient EPSCs, as shown in Fig. 7A. At the most negative potentials where NMDA-receptor-gated channels are blocked by Mg^{2+} , CNQX suppressed nearly all light-evoked current. At more positive potentials the fast component was blocked but the slow component of

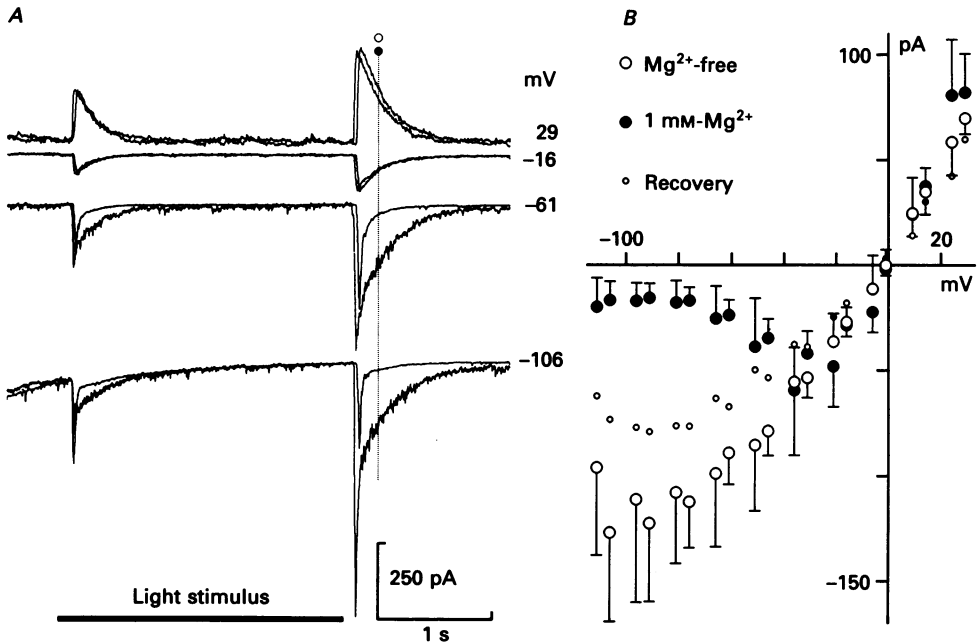


Fig. 6. *A*, transient EPSCs evoked by light (6×10^{17} photons $m^{-2} s^{-1}$) in control or Mg^{2+} -free saline. The records in Mg^{2+} -free saline are the larger of each pair at hyperpolarized voltages and have a shorter latency at all voltages. *B*, mean, normalized, late $I-V$ curves determined from two on and fifteen off transient EPSCs. $I-V$ curves were measured at latencies of 171–420 ms from the onset or cessation of a light step. The open circles are from data obtained in Mg^{2+} -free saline. Retinal slices were prepared and superfused for at least 30 min in Mg^{2+} -free saline prior to the start of the experiment. The filled circles are from data obtained after superfusion of control saline (1 mM- Mg^{2+}) for 4 min. The recovery $I-V$ curve was determined from light responses recorded 20 min after superfusion of Mg^{2+} -free saline.

the response was unaffected. The mean, normalized $I-V$ curves of nine cells (Fig. 7B and C) reinforce these observations. Prior to addition of CNQX, the $I-V$ curve measured at the early time had a positive slope conductance between -30 and 30 mV and near-zero slope conductance negative to -30 mV (\square). CNQX abolished most of this current but the $I-V$ curve of the residual response showed a small peak inward current close to -36 mV (\blacksquare), suggesting activation of NMDA receptors. The late $I-V$ curve (Fig. 7C) was unchanged by CNQX and had the typical negative slope conductance of an NMDA-receptor-gated current (Mayer *et al.* 1984; Nowak *et al.* 1984; Mayer & Westbrook, 1985).

Although the most apparent and consistent action of $1 \mu M$ -CNQX was to abolish selectively the fast component of transient EPSCs, CNQX had other effects. In some

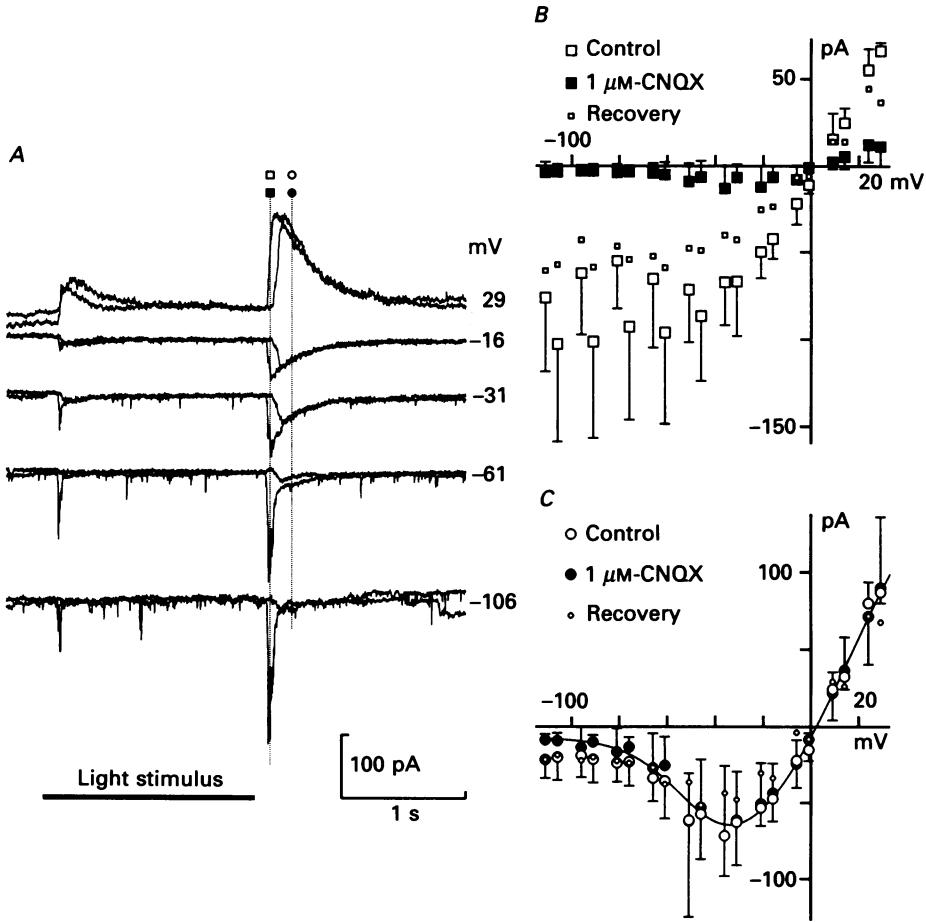


Fig. 7. *A*, transient EPSCs evoked by light (6×10^{17} photons $\text{m}^{-2} \text{s}^{-1}$) both before and during application of 1 μM -CNQX. The control traces have larger amplitude responses at negative potentials and have shorter response latencies at all potentials. *B*, mean, normalized, early $I-V$ curves from eight on and eight off transient EPSCs are plotted. The $I-V$ curves were measured at latencies of 120–200 ms from the onset or cessation of a light step. The effects of CNQX on on transient EPSCs were not different from the effects on off transient EPSCs. *C*, mean, normalized late $I-V$ curves determined from the same transient EPSCs as in *B*. These $I-V$ curves were measured at latencies of 220–340 ms from the onset or cessation of a light step. The continuous line was calculated from a two-barrier, one-site model (Hille, 1984) of the NMDA-receptor channel. For monovalent cations the free energies of the outer barrier, binding site and inner barrier were $10.9RT$, $3.8RT$ and $10.4RT$, where R is the gas constant and T is absolute temperature. For Mg^{2+} the free energies of the outer barrier, binding site and inner barrier were $16.4RT$, $-2.9RT$ and $23.4RT$. The electrical distance of the binding site from the outside surface of the membrane was 99%. Total monovalent cation concentration was assumed to be 120 mM on both sides of the membrane. Mg^{2+} concentration was assumed to be 1 mM outside and 0 mM inside.

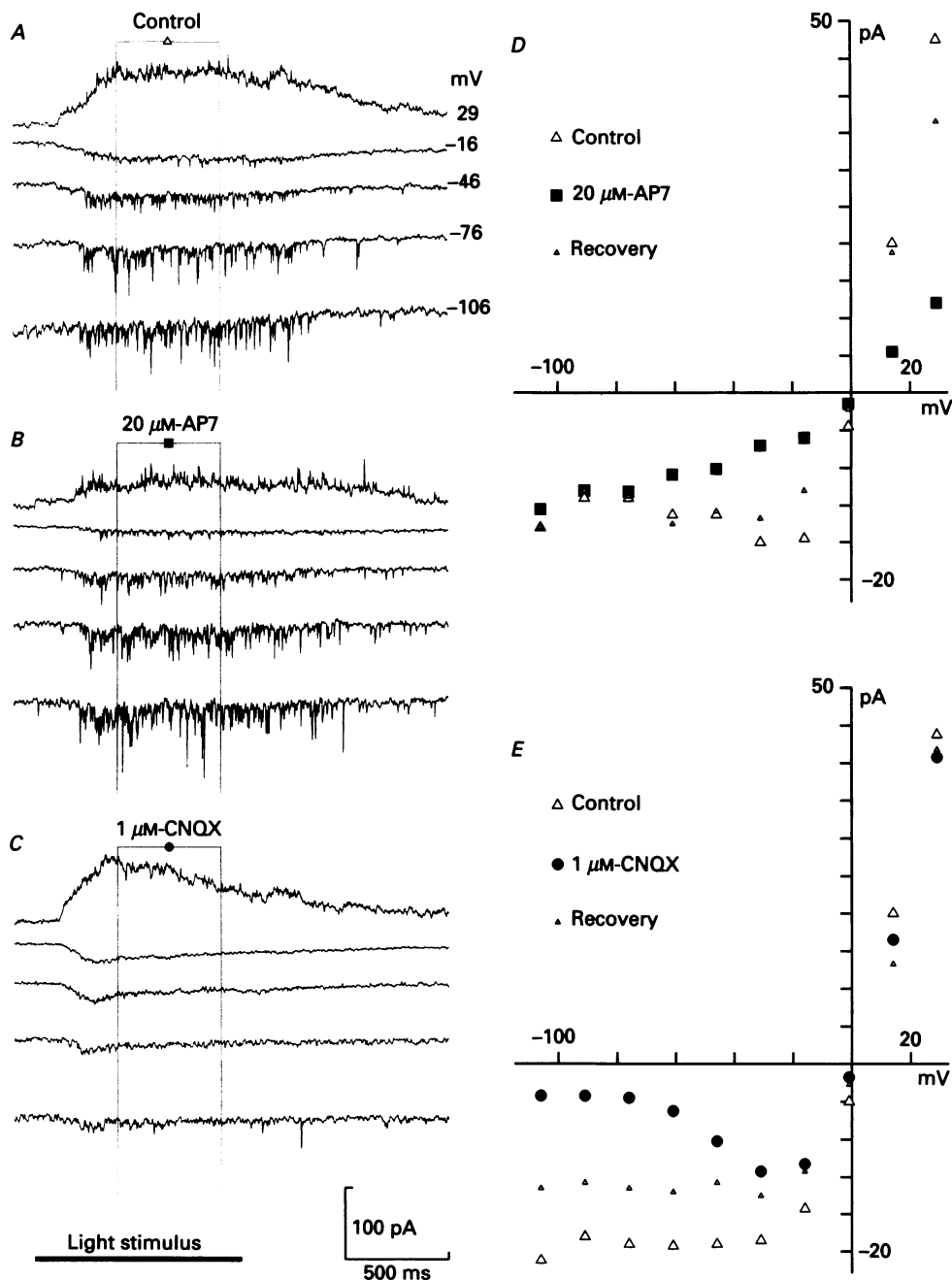


Fig. 8. Light-evoked postsynaptic currents of an on-centre ganglion cell recorded under three conditions: *A*, superfusion with control saline; *B*, addition of 20 μM -AP7 to control saline; *C*, addition of 1 μM -CNQX to the control saline. The timing of the stimulus (6×10^{19} photons $\text{m}^{-2} \text{s}^{-1}$) is indicated by the bar below *C*. Traces were recorded at the potentials listed to the right of *A*. *D*, mean I - V curves of two sustained EPSCs before (Δ), during (\blacksquare) and after (\blacktriangle) application of AP7. Evoked current was calculated as the difference between the mean current during a half-second portion of the light response and

cells CNQX caused a slight increase in the amplitude of the NMDA-receptor-mediated component of transient EPSCs; in other cells it reduced the amplitude slightly.

Sometimes CNQX also caused an increase in the latency of light responses (Fig. 7A, off response). One manifestation of the latency shift is a seemingly paradoxical finding in which the near-zero slope conductance of the early, control I - V curve (Fig. 7B, \square) suggests that the early current had a substantial NMDA-receptor-mediated component, yet in CNQX only a small NMDA-receptor-mediated current was seen (Fig. 7B, \blacksquare). This discrepancy is an artifact of measuring currents at a fixed time point with respect to the stimulus. None the less, the predominant effect of CNQX was to block selectively the fast component of transient EPSCs.

In the two cases tested, concomitant application of CNQX and AP7 completely abolished the excitatory inputs to on-off ganglion cells.

The components of transient EPSCs and agonist-evoked currents have similar reversal potentials

Figure 2C shows I - V curves for NMDA responses and the slow component of transient EPSCs measured in the same cells ($n = 3$). The reversal potential of NMDA-evoked currents was 0.2 ± 2.9 mV and of the slow component, 2.2 ± 1.7 mV. Both sets of curves exhibited negative slope regions. For the three on-off cells in which responses to both light and quisqualate or kainate were recorded, the reversal potential of agonist-evoked responses was -2.2 ± 2.5 mV and of the fast component, 0.1 ± 6.3 mV (Fig. 3A and B).

In summary, these data are consistent with the idea that in on-off ganglion cells there is a fast, non-NMDA-gated component of transient EPSCs that is AP7 resistant and CNQX sensitive. There also appears to be a slower, NMDA-receptor-gated component of light-evoked transient EPSCs that is CNQX resistant but is antagonized by AP7 and blocked by Mg^{2+} at hyperpolarized potentials.

NMDA and non-NMDA receptors mediate light-evoked sustained EPSCs in on ganglion cells

The same strategies of examining light-evoked inputs at a number of potentials and of using specific pharmacological agents were employed to characterize the sustained EPSC in on ganglion cells. The I - V curve of the sustained EPSC in control solutions was similar to that observed for the early phase of transient EPSCs (Fig. 8D, \triangle). Positive to -15 mV, the I - V curve had a positive slope conductance, while negative to this voltage the slope conductance was close to zero. This I - V curve, intermediate in shape to I - V curves obtained from pure NMDA- and non-NMDA-receptor-mediated responses, suggested that a mixed population of acidic amino acid receptors may also mediate the sustained EPSC. AP7 and CNQX were used to test this hypothesis.

the current in the dark. E , mean I - V curves of the same two sustained EPSCs before (\triangle), during (\bullet) and after (Δ) application of CNQX. The control I - V curves in each panels (D and E) were measured immediately preceding application of the antagonist under consideration and, hence, differ.

Figure 8B shows that 20 μM -AP7 blocked a significant portion of the current at the most depolarized potentials. A noisy component of the sustained EPSC was not blocked by AP7. This component had a more nearly linear I - V curve, with a positive slope over the entire voltage range (Fig. 8D, ■), expected of a response mediated by non-NMDA receptors. CNQX at 1 μM blocked the noisy component of the current but did not block the less-noisy component (Fig. 8C) which had an I - V curve characteristic of responses mediated by NMDA receptors (Fig. 8E, ●). Thus, the sustained EPSC appears to be mediated by concomitant activation of NMDA and non-NMDA receptors.

One on ganglion cell was tested for the effects of changing external Mg^{2+} concentration. The I - V curve of the sustained EPSC, which had a near-zero slope conductance between -100 and -15 mV in normal saline, had a positive slope conductance over this potential range in Mg^{2+} -free saline, consistent with the Mg^{2+} sensitivity of NMDA receptors.

The kinetics of responses mediated by each receptor type are similar in on-off and on ganglion cells

Figure 9A and B shows the responses of an on and an on-off ganglion cell to steps of light recorded in AP7 and CNQX, at a potential of -31 mV. Figure 9C and D shows, on an expanded time scale, the onset of each cell's response. The non-NMDA-receptor-mediated portion of each response consisted of a summation of fast (< 10 ms) inward current events. The NMDA-receptor-mediated portion lacked such discrete events.

Figure 9E shows, on an expanded time scale, the off response of the on-off ganglion cell. As with the on response of this cell, the non-NMDA-receptor-mediated portion of the response consisted of numerous fast current events. In this case, the higher frequency of these events led to considerable summation.

Figure 9E also compares the overall times-to-peak and decay time constants of the components mediated by each receptor. The non-NMDA-receptor-mediated input (top) rose to a peak in 25 ms and decayed e-fold in about 17 ms while the slower NMDA-receptor-mediated input (bottom) rose to a peak in 75 ms and decayed e-fold in 270 ms. Averages of eight cells showed a time-to-peak and decay time of 28 ± 10 ms and 43 ± 20 ms for the fast component; averages of five cells showed a time-to-peak and decay time of 110 ± 45 ms and 209 ± 35 ms for the slow component.

Internal fluoride and inhibitory amino acid-receptor antagonists are not sources of artifact

Two aspects of the experimental design merit attention as possible sources of artifact. Fluoride was chosen as the predominant anion of the patch-pipette filling solution because it greatly increased the yield of high-quality tight-seal, whole-cell recordings. As a control for possible artifacts due to fluoride, experiments were performed with chloride substituted for fluoride. Both the slow and fast components of the response were unchanged with this internal solution relative to the results reported above.

The antagonists strychnine and bicuculline methobromide were used to block inhibitory currents and thus simplify the analysis of the remaining excitatory inputs

to ganglion cells. The slow component, in particular, would have been difficult to study in the presence of concomitant inhibitory inputs. As a control for possible presynaptic effects of the GABA- and glycine-receptor antagonists on transient EPSCs, a few experiments were performed without them. For these experiments,

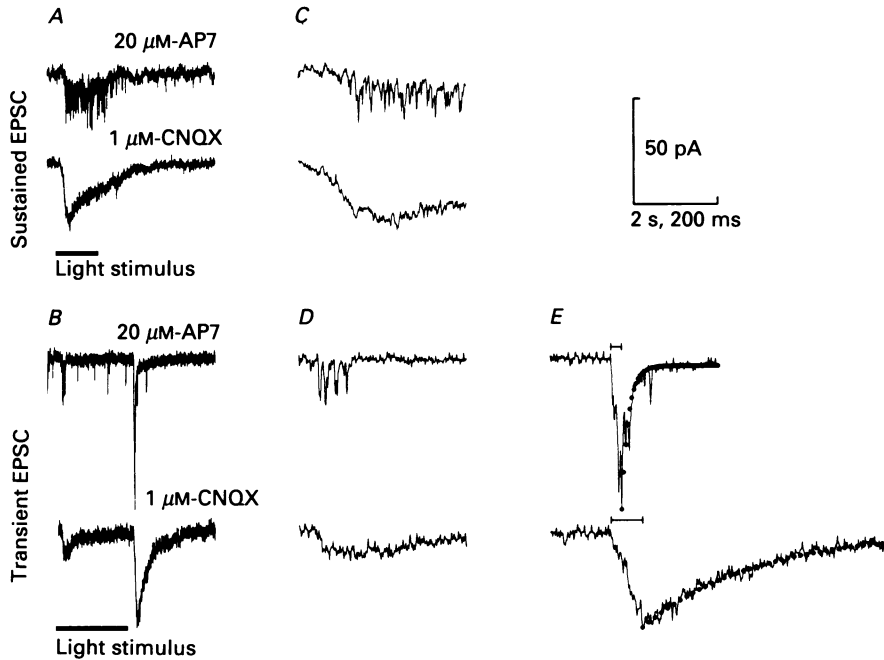


Fig. 9. *A*, sustained EPSC recorded at a potential of -31 mV in the presence of AP7 (top trace) or CNQX (bottom trace). Light intensity was 6×10^{18} photons $m^{-2} s^{-1}$. *B*, transient EPSCs recorded at a potential of -31 mV in the presence of AP7 (top trace) or CNQX (bottom trace). Light intensity was 6×10^{17} photons $m^{-2} s^{-1}$. *C-E*, portions of the same EPSCs, displayed on an expanded time scale. In *C* and *D*, the beginning of the trace marks the onset of the light stimulus; in *E*, it marks the cessation of the stimulus. The two horizontal markers above the traces (*E*) show the times-to-peak of the components. The fast-component time-to-peak was 25 ms; the slow-component time-to-peak, 75 ms. The small, filled circles show the single-exponential decay functions that best fitted the falling phases of the responses. The fast-component decay time constant was 17 ms; the slow-component decay time constant, 267 ms. Time calibration: *A* and *B*, 2 s; *C-E*, 200 ms.

Mg^{2+} -free saline was used to enhance the slow component of transient EPSCs at hyperpolarized potentials. In this case, too, both fast and slow components of transient EPSCs were observed. Although the components could not be distinguished on the basis of their $I-V$ curves in Mg^{2+} -free saline, AP7 did block only the slow component.

DISCUSSION

In these experiments, we observed that the excitatory input to both on and on-off retinal ganglion cells was mediated by a mixed population of postsynaptic acidic amino acid receptors. In on-off ganglion cells, non-NMDA receptors mediated a fast component of transient EPSCs and NMDA receptors mediated a slow component.

Likewise, in on ganglion cells, non-NMDA receptors mediated a noisy component of the sustained EPSC and NMDA receptors mediated a less noisy component. Thus in Fig. 10, a model of the acidic amino acid-receptor-mediated pathways from photoreceptors to on and on-off ganglion cells in salamander, NMDA (○) and non-

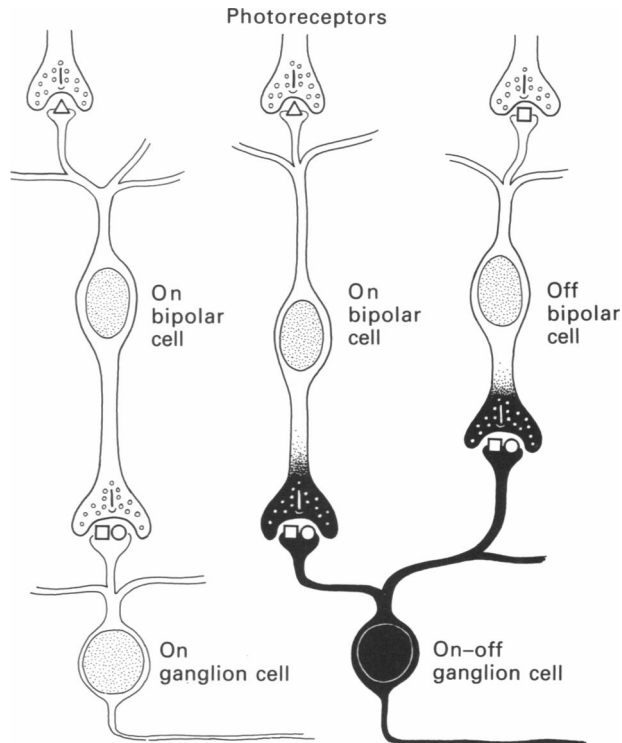


Fig. 10. A model of acidic amino acid-receptor-mediated neurotransmission in radial (photoreceptor–bipolar–ganglion cell) pathways of the salamander retina. The darkly shaded cytoplasm of the on bipolar cell synaptic terminal (middle) and the off bipolar cell terminal (right) indicates that these terminals release transmitter transiently. Likewise, the dark shading of the on-off ganglion cell indicates its transient response to sustained illumination. For further explanation, see the text. Glutamate receptor types: □, non-NMDA; ○, NMDA; △, AP4.

NMDA (□) receptors are shown side-by-side on both types of ganglion cell. The arrangement of receptors on the dendrites of bipolar cells conforms to the evidence of Slaughter & Miller (1981, 1983*b*) and Shiells, Falk & Naghshineh (1981): on bipolar cells possess 2-amino-4-phosphonobutanoate (AP4) receptors (△) and off bipolar cells possess non-NMDA receptors (□).

NMDA and non-NMDA receptors mediate the excitatory input to retinal ganglion cells

In contrast to previous studies of the excitatory inputs to retinal ganglion cells (Slaughter & Miller, 1983*b*; Lukasiewicz & McReynolds, 1985; Coleman *et al.* 1986; Coleman & Miller, 1988; Massey & Miller, 1988; Coleman & Miller, 1989), this study conclusively demonstrates that a portion of the light-evoked responses of both on-off

and on ganglion cells is mediated by synaptic NMDA receptors (Fig. 10, ○). Light-evoked conductances had many of the hallmarks of NMDA-receptor-mediated responses in both cell types: I - V curves with regions of negative slope below -40 mV, relief of voltage-dependent block by low external Mg^{2+} and sensitivity to AP7. Previous studies relied on intracellular micropipette voltage recordings of mixed excitatory and inhibitory postsynaptic responses. Interpretation of these recordings was made even more difficult by the voltage-dependent conductances of ganglion cells. In the present study, we were able to isolate EPSCs from both inhibitory and voltage-gated currents using inhibitory amino acid-receptor antagonists (Fig. 4A-C) and the voltage-clamp technique.

We also postulate that non-NMDA receptors mediate the remainder of the excitatory input to on and on-off retinal ganglion cells (Fig. 10, □) since CNQX, a selective non-NMDA-receptor antagonist, eliminated that portion of the current not mediated by NMDA receptors. This conclusion, however, is less certain than that concerning NMDA receptors because non-NMDA-receptor-gated conductances have no unambiguous identifying characteristics and because light-evoked excitation of ganglion cells involves at least two synapses. One logical alternative is that the receptor mediating the fast component of transient EPSCs and the noisy component of sustained EPSCs could be an as yet unidentified type. In this scenario, CNQX would have its action at the acidic amino acid receptors on the dendrites of bipolar cells. Opposed to this alternative is the demonstrated presence of non-NMDA receptors on retinal ganglion cells (Fig. 3). Furthermore, our results strongly resemble those obtained with cultured hippocampal neurones. Stimulation of one cultured neurone evokes a monosynaptic response in a second neurone that consists of both a fast and a slow component (Forsythe & Westbrook, 1988). Bekkers & Stevens (1989) have demonstrated that the fast component is mediated by postsynaptic non-NMDA receptors by blocking this component of the monosynaptic response with CNQX. Thus, NMDA and non-NMDA receptors probably co-exist on the postsynaptic membrane of retinal ganglion cells as on other neurones.

Displaced amacrine cells may also receive concomitant NMDA and non-NMDA inputs

Our recordings were from cells of the ganglion cell layer of tiger salamander retina. Figure 10 shows only ganglion cells in this layer but up to 50% of the cells in the ganglion cell layer may be displaced amacrine cells in urodele species (Turner *et al.* 1978; Ball & Dickson, 1983). Thus, several of the ninety-four cells that we studied were likely to have been displaced amacrine cells. In fact, preliminary work suggests that amacrine cells with cell bodies in the inner nuclear layer also possess a mixed population of NMDA and non-NMDA receptors (D. B. Dixon & D. R. Copenhagen, personal communication).

Do on-off ganglion cells receive direct input from bipolar cells?

A more speculative element of the model shown in Fig. 10 is the direct connection between bipolar cells and the on-off ganglion cell; only indirect evidence supports these synaptic interactions. The chief objection to these interactions is that the on-off ganglion cell response to light bears little resemblance to the on and off bipolar cell responses. Marchiafava & Torre (1978) have suggested that the terminals of some

bipolar cells release transmitter in a transient fashion despite the sustained nature of the response recorded from the bipolar cell soma. This hypothesis is represented graphically in Fig. 10 by the shading in the bipolar synaptic terminals. The on and off bipolar cell terminals that are purported to release transmitter in a transient fashion are darkly shaded. The terminal of the sustained-releasing on bipolar cell is unshaded.

Maguire, Lukasiewicz & Werblin (1989) have recently suggested a mechanism for transient release: feedback inhibition of bipolar cell transmitter release by GABA_B receptors. This issue will probably be resolved only by the demonstration of short-latency postsynaptic responses in an on-off ganglion cell following depolarization of an identified bipolar cell.

The presynaptic neurone probably releases transmitter in discrete packets

We observed that the non-NMDA-receptor-mediated components of retinal ganglion cell EPSCs were more rapid than their NMDA-receptor-mediated counterparts. In on-off ganglion cells, for example, the non-NMDA-receptor-mediated component of off transient EPSCs rose to a peak in an average of 28 ms and decayed e-fold in an average of 43 ms. The NMDA-receptor-mediated component rose to a peak in an average of 110 ms and decayed e-fold in an average of 209 ms.

Although similar to the results seen in a number of other preparations (Wigström *et al.* 1985; Dale & Roberts, 1985; Forsythe & Westbrook, 1988; Bekker & Stevens, 1989), these results are quantitatively different. For example, the fast component of EPSCs evoked in cultured central neurones decayed e-fold in under 4 ms (Forsythe & Westbrook, 1988). We attribute much of the disparity to differences in the two preparations. EPSCs in cultured central neurones were synchronously evoked by single action potentials in a presynaptic neurone. In contrast, transient EPSCs were evoked by light stimulation via photoreceptors and bipolar cells, neither of which fires action potentials.

The fast component of transient EPSCs appeared to consist of multiple, overlapping rapid events (Fig. 9E, upper trace), each similar in time course to the fast component observed by Forsythe & Westbrook (1988). We interpret these rapid events as the postsynaptic responses to release of discrete packets of transmitter. These packets may be the contents of individual synaptic vesicles or the contents of groups of vesicles released from an individual presynaptic terminal. In this interpretation, the overall time course of the fast component of transient EPSCs is the result of asynchronous release of packets over a period of tens of milliseconds. Likewise, the noisy behaviour of the non-NMDA-receptor-mediated component of sustained EPSCs (Fig. 9C, upper trace) can be explained as the postsynaptic response to a stream of discrete transmitter packets released continuously by on bipolar cells, depolarized by light. Thus, the differences between non-NMDA-receptor-mediated EPSCs in on ganglion cells, in on-off ganglion cells and in mouse cultured neurones are probably the result of differences in the time course of presynaptic transmitter release.

The NMDA-receptor-mediated components of ganglion cell EPSCs (Fig. 9C, D and E, lower traces) displayed no constituent rapid events. Similar behaviour has been observed by Dale & Roberts (1985). They recorded EPSPs in motoneurones of

Xenopus spinal cord evoked by extracellular stimulation of individual axons. In response to single stimuli, EPSPs consisted of mixed fast and slow components. In response to 20 Hz stimulus trains, however, the slow components added to produce a sustained background depolarization while the fast components were visible as phasic components superimposed on the sustained depolarization. Dale & Roberts (1985) concluded that the sustained depolarization was due to substantial temporal summation of the individual slow components of the response, slow components whose duration was far longer than the interstimulus interval. Because EPSCs were not evoked monosynaptically in our experiments, we do not know the duration of the slow component evoked by a single stimulus. None the less, the smooth nature of NMDA-receptor-mediated responses in ganglion cells is probably also due to temporal summation of individual slow postsynaptic currents. Still unexplained is the molecular basis of the difference in kinetics of NMDA- and non-NMDA-receptor-mediated components of EPSCs.

The action of CNQX suggests a difference between excitatory synapses in the inner and outer plexiform layers

Light-evoked signals traverse photoreceptor-to-bipolar cell synapses before reaching the ganglion cell; therefore, it is important to assess the effects of AP7 and CNQX at these synapses. Transient on and off responses could be recorded in the presence of either antagonist. For responses mediated by on bipolar cells, this result is not surprising as the acidic amino acid receptor found on this cell is the AP4 receptor (Fig. 10, Δ), a receptor with a pharmacology substantially different than those of NMDA and non-NMDA receptors (Shiells *et al.* 1981; Slaughter & Miller, 1981). The resistance of the slow component of off transient EPSCs to CNQX raises some questions, as CNQX might be expected to antagonize the off bipolar cell acidic amino acid receptor. Either transfer through this synapse involves receptors different from the non-NMDA receptor of ganglion cells, or CNQX is less effective at this synapse because of higher synaptic glutamate concentrations. Recent work with D-O-phosphoserine supports the former possibility (Coleman & Miller, 1989). This agent antagonized the excitatory responses of amacrine and ganglion cells in mudpuppy retina, yet was ineffective at blocking transmission through the photoreceptor-to-off-bipolar cell synapse.

We thank Dr Don Dixon for critically reading the manuscript and Joan Weddell for help with the figures. S.M. was a trainee of the Medical Scientist Training Program at the University of California, San Francisco (GM07618). W. R. T. was a Fight-for-Sight post-doctoral fellow. Our work was supported by grants from the National Eye Institute (EY01869, to D. R. C.) and the National Society to Prevent Blindness (to S. M.).

REFERENCES

- AIZENMAN, E., FROSCHE, M. P. & LIPTON, S. A. (1988). Responses mediated by excitatory amino acid receptors in solitary retinal ganglion cells from rat. *Journal of Physiology* **396**, 75–91.
- ASCHER, P. & NOWAK, L. (1988). The role of divalent cations in the N-methyl-D-aspartate responses of mouse central neurones in culture. *Journal of Physiology* **399**, 247–266.
- BALL, A. K. & DICKSON, D. H. (1983). Displaced amacrine and ganglion cells in the newt retina. *Experimental Eye Research* **36**, 199–213.

- BEKKERS, J. M. & STEVENS, C. F. (1989). NMDA and non-NMDA receptors are co-localized at individual excitatory synapses in cultured rat hippocampus. *Nature* **341**, 230–233.
- BELGUM, J. H., DVORAK, D. R. & McREYNOLDS, J. S. (1984). Strychnine blocks transient but not sustained inhibition in mudpuppy retinal ganglion cells. *Journal of Physiology* **354**, 273–286.
- COLEMAN, P. A., MASSEY, S. C. & MILLER, R. F. (1986). Kynurenic acid distinguishes kainate and quisqualate receptors in the vertebrate retina. *Brain Research* **381**, 172–175.
- COLEMAN, P. A. & MILLER, R. F. (1988). Do *N*-methyl-D-aspartate receptors mediate synaptic responses in the mudpuppy retina? *Journal of Neuroscience* **8**, 4728–4733.
- COLEMAN, P. A. & MILLER, R. F. (1989). Kainate receptor-mediated synaptic currents in mudpuppy inner retinal neurons reduced by D-*O*-phosphoserine. *Journal of Neurophysiology* **62**, 495–500.
- DALE, N. & ROBERTS, A. (1985). Dual-component amino-acid-mediated synaptic potentials: excitatory drive for swimming in *Xenopus* embryos. *Journal of Physiology* **363**, 35–59.
- FORSYTHE, I. A. & WESTBROOK, G. L. (1988). Slow excitatory postsynaptic currents mediated by *N*-methyl-D-aspartate receptors on cultured mouse central neurones. *Journal of Physiology* **396**, 515–533.
- FRUMKES, T. E., MILLER, R. F., SLAUGHTER, M. & DACHEUX, R. F. (1981). Physiological and pharmacological basis of GABA and glycine action on neurons of mudpuppy retina. III. Amacrine-mediated inhibitory influences on ganglion cell receptive-field organization: a model. *Journal of Neurophysiology* **45**, 783–804.
- HILLE, B. (1984). *Ionic Channels of Excitable Membranes*. Sinauer Associates, Sunderland, MA, USA.
- HOFFMAN, R. & GROSS, L. (1975). The modulation contrast microscope. *Nature* **254**, 586–588.
- HONORÉ, T., DAVIES, S. N., DREJER, J., FLETCHER, E. J., JACOBSEN, P., LODGE, D. & NIELSEN, F. E. (1988). Quinoxalinediones: potent competitive non-NMDA glutamate receptor antagonists. *Science* **241**, 701–703.
- LUKASIEWICZ, P. D. & McREYNOLDS, J. S. (1985). Synaptic transmission at *N*-methyl-D-aspartate receptors in the proximal retina of the mudpuppy. *Journal of Physiology* **367**, 99–115.
- LUKASIEWICZ, P. & WERBLIN, F. (1988). A slowly inactivating potassium current truncates spike activity in ganglion cells of the tiger salamander retina. *Journal of Neuroscience* **8**, 4470–4481.
- MAGUIRE, G., LUKASIEWICZ, P. & WERBLIN, F. (1989). Amacrine cell interactions underlying the response to change in the tiger salamander retina. *Journal of Neuroscience* **9**, 726–735.
- MARCHIAFAVA, P. L. & TORRE, V. (1978). The responses of amacrine cells to light and intracellularly applied currents. *Journal of Physiology* **276**, 83–102.
- MARTY, A. & NEHER, E. (1983). Tight-seal whole-cell recording. In *Single-Channel Recording*, ed. SAKMANN, B. & NEHER, E., pp. 107–122. Plenum Press, New York.
- MASSEY, S. C. & MILLER, R. F. (1988). Glutamate receptors of ganglion cells in the rabbit retina: evidence for glutamate as a bipolar cell transmitter. *Journal of Physiology* **405**, 635–655.
- MAYER, M. L., VYKLYCKY, L. JR & WESTBROOK, G. L. (1989). Modulation of excitatory amino acid receptors by group IIB metal cations in cultured mouse hippocampal neurones. *Journal of Physiology* **415**, 329–350.
- MAYER, M. L. & WESTBROOK, G. L. (1984). Mixed-agonist action of excitatory amino acids on mouse spinal cord neurones under voltage clamp. *Journal of Physiology* **354**, 29–53.
- MAYER, M. L. & WESTBROOK, G. L. (1985). The action of *N*-methyl-D-aspartic acid on mouse spinal neurones in culture. *Journal of Physiology* **361**, 65–90.
- MAYER, M. L. & WESTBROOK, G. L. (1987). Permeation and block of *N*-methyl-D-aspartic acid receptor channels by divalent cations in mouse cultured central neurones. *Journal of Physiology* **394**, 501–527.
- MAYER, M. L., WESTBROOK, G. L. & GUTHRIE, P. B. (1984). Voltage-dependent block by Mg^{2+} of NMDA responses in spinal cord neurones. *Nature* **309**, 261–263.
- MILLER, R. F., DACHEUX, R. F. & FRUMKES, T. E. (1977). Amacrine cells in *Necturus* retina: evidence for independent γ -aminobutyric acid and glycine-releasing neurons. *Science* **198**, 748–750.
- MILLER, R. F., FRUMKES, T. E., SLAUGHTER, M. & DACHEUX, R. F. (1981). Physiological and pharmacological basis of GABA and glycine action on neurones of mudpuppy retina. II. Amacrine and ganglion cells. *Journal of Neurophysiology* **45**, 764–782.
- MITTMAN, S., FLAMING, D. G., COPENHAGEN, D. R. & BELGUM, J. H. (1987). Bubble pressure measurement of micropipet tip outer diameter. *Journal of Neuroscience Methods* **22**, 161–166.

- NOWAK, L., BREGESTOVSKI, P., ASCHER, P., HERBET, A. & PROCHIANTZ, A. (1984). Magnesium gates glutamate-activated channels in mouse central neurones. *Nature* **307**, 462–465.
- OLVERMAN, H. J., JONES, A. W. & WATKINS, J. C. (1984). L-Glutamate has higher affinity than other amino acids for [³H]-D-AP5 binding sites in rat brain membranes. *Nature* **307**, 460–462.
- PERRY, V. H. (1979). The ganglion cell layer of the retina of the rat: a Golgi study. *Proceedings of the Royal Society B* **204**, 363–375.
- SHIELLS, R. A., FALK, G. & NAGHSHINEH, S. (1981). Action of glutamate and aspartate analogues on rod horizontal and bipolar cells. *Nature* **294**, 592–594.
- SLAUGHTER, M. M. & MILLER, R. F. (1981). 2-Amino-4-phosphonobutyric acid: a new pharmacological tool for retina research. *Science* **211**, 182–185.
- SLAUGHTER, M. M. & MILLER, R. F. (1983a). Bipolar cells in the mudpuppy retina use an excitatory amino acid neurotransmitter. *Nature* **303**, 537–538.
- SLAUGHTER, M. M. & MILLER, R. F. (1983b). The role of excitatory amino acid transmitters in the mudpuppy retina: an analysis with kainic acid and *N*-methyl-D-aspartate. *Journal of Neuroscience* **3**, 1701–1711.
- TURNER, J. E., DELANEY, R. K. & POWELL, R. E. (1978). Retinal ganglion cell response to axotomy in the regenerating visual system of the newt (*Triturus viridescens*): an ultrastructural morphometric analysis. *Experimental Neurology* **62**, 444–462.
- WERBLIN, F. S. (1978). Transmission along and between rods in the tiger salamander retina. *Journal of Physiology* **280**, 449–470.
- WIGSTRÖM, H., GUSTAFSSON, B. & HUANG, Y.-Y. (1985). A synaptic potential following single volleys in the hippocampal CA1 region possibly involved in the induction of long-lasting potentiation. *Acta physiologica scandinavica* **124**, 475–478.
- WU, S. M. (1987). Synaptic connections between neurons in living slices of the larval tiger salamander retina. *Journal of Neuroscience Methods* **20**, 139–149.
- WUNK, D. F. & WERBLIN, F. S. (1979). Synaptic inputs to the ganglion cells in the tiger salamander retina. *Journal of General Physiology* **73**, 265–286.
- YAMADA, K. A., DUBINSKY, J. M. & ROTHMAN, S. M. (1989). Quantitative physiological characterization of a quinoxalinedione non-NMDA receptor antagonist. *Journal of Neuroscience* **9**, 3230–3236.